ELSEVIER

Applied Catalysis A: General 172 (1998) 85–95

APPLIED CATALYSIS A: GENERAL

Different adsorbate binding mechanisms of hydrocarbons: Theoretical studies for Cu(111)–C_2H_2 and Cu(111)–C_2H_4

M. Witko[a], K. Hermann[b,*]

[a] *Institute of Catalysis and Surface Chemistry, Polish Academy of Sciences, ul. Niezapominajek, 30239 Cracow, Poland*
[b] *Fritz–Haber-Institut der MPG, Faradayweg 4–6, D-14195 Berlin, Germany*

Received 16 January 1998; received in revised form 19 March 1998; accepted 20 March 1998

Abstract

Experimental results for acetylene and ethylene adsorption on metal surfaces indicate qualitatively different adsorbate binding mechanisms, depending on the adsorbate and substrate material. Experiments on Cu(111)–C_2H_2 identify a strongly distorted adsorbate while the adsorption energy is small. In contrast, recent experiments on Cu(111)–C_2H_4 have identified a weakly physisorbed adsorbate without noticeable structural changes. The qualitatively different binding behavior between C_2H_2 and C_2H_4 with Cu(111) has been examined by ab-initio density functional theory (DFT) cluster studies. Restricted geometry optimizations yield potential energy curves $E(z)$ which exhibit two minima for both adsorbates. The outer minimum refers to an undistorted adsorbate (indicating a physisorbed state) while the inner minimum yields a strongly distorted adsorbate (confirming a competitive binding state). Qualitative differences between the inner and outer potential minima of the two systems can explain their different behavior. The $E(z)$ curves can also rationalize why in experiments for Cu(111)–C_2H_2 and Cu(111)–C_2H_4 only one of the two adsorbate states has been verified so far. However, the present calculations suggest to further look for experiments where both adsorbate states can be prepared.

Keywords: Adsorbate binding; Metals; Hydrocarbons; Density functional theory; Cluster model

1. Introduction

Catalytically activated reactions of hydrocarbons at transition-metal surfaces start with the adsorption of the organic reactant(s) at the catalyst surface. Here, sophisticated experimental techniques allow one to identify the local adsorption geometry (structural parameters of the adsorbed molecules) before, and after, a catalytic reaction has occurred which can yield information about possible reaction pathways. The catalyst surface is the stage for various processes such as geometric/electronic restructuring of the adsorbate, bond formation and reaction between adsorbates as well as with the substrate, and reconstruction of the substrate surface. Therefore, understanding basic mechanism of any catalytic reaction requires a detailed knowledge about electronic and geometric properties of both, the catalyst surface and the reacting molecules. As a next step, the characterization of transition complexes formed from the adsorbates and respective substrate atoms is needed. This gives information concerning bond making/breaking in the

*Corresponding author. Tel.: 0049-30-84134812; fax: 0049-30-84134701; e-mail: hermann@fhi-berlin.mpg.de

0926-860X/98/$19.00
PII S0926-860X(98)00108-2

adsorbate as well as about changes in the reactivity as a consequence of modified bonds. All above parameters influence reaction pathways leading to the desired reaction products.

The reacting hydrocarbon molecule may adsorb at the surface by forming bonds of different strength and character with the surface. If the binding energy is low (<0.1 eV per adsorbing molecule) and the molecule undergoes no geometric changes then it is physisorbed. Here, binding is connected with the weak adsorbate–substrate coupling of physical origin (e.g. Van der Waals type) and leaves the electronic structure of the adsorbate almost unchanged. Higher binding energies (>0.7 eV up to several eV per adsorbing molecule) indicate that the molecule is chemisorbed at the surface. This process is characterized by a strong adsorbate–substrate interaction of chemical origin (formation of covalent or ionic chemical bonds). In this case, both the electronic and geometric structures of the molecule are affected by adsorption.

A full microscopic description of the adsorption process has to take into account the local adsorbate–substrate interaction as well as changes in the intramolecular binding of the adsorbate. The total energy, characterizing the global surface interaction of the molecular adsorbate, combines the contributions from energies connected with different surface binding (Van der Waals, ionic, covalent) with those from changes in the intramolecular adsorbate binding. If adsorption is only accompanied by minor changes in the intramolecular structure, then adsorption energetics are determined only by the adsorbate - substrate binding. However, intramolecular binding may be strongly affected by adsorption resulting in a major geometric rearrangement of the adsorbate. Thus, the corresponding energy contributions cannot be neglected and the adsorption energetics may not reflect the local adsorbate-substrate bond strength. An obvious example is given by dissociative adsorption where the adsorbate loses its identity near the surface [1,2]. Other examples are those where the energy required for geometric rearrangements in the adsorbing molecule can be overcompensated by the energy gain due to local bond formation between the distorted adsorbate molecule and the substrate surface (competitive binding scheme). As a result, the global surface interaction of the molecular adsorbate may be weak but cannot be described by physisorption.

From the experimental results, as well as theoretical cluster studies discussed below, the adsorption of small organic molecules at metal surfaces is found to be determined by different binding mechanisms depending on the adsorbate and substrate material. In the present theoretical study based on cluster model calculations on the adsorbate Cu(111)–C_2H_2 and Cu(111)–C_2H_4 systems, we point out that two mechanisms, competitive binding and weak physisorption, can occur in the same system. This theoretical result adds another detail to the rather complex adsorption and reaction pathways of hydrocarbons on metal substrates and may stimulate further experimental work on these systems.

Section 2 reviews recent experimental and theoretical results referring to geometric and electronic properties of small hydrocarbons at metal surfaces. Section 3 gives a few basic-theoretical details of the present work while Section 4 presents results and discussion. Finally, in Section 5, we summarize our conclusions from the present calculations.

2. Adsorption and binding of C_2H_2 and C_2H_4 at metal surfaces

2.1. Experimental findings

Acetylene (C_2H_2) adsorption at metal surfaces is characterized by overall small adsorption energies and requires rather low temperatures in order to stabilize the adsorbate near the surface [3–6]. On the other hand, photoelectron diffraction (PED) experiments for C_2H_2 on Cu(111) [3] and Ni(111) [4,5] as well as X-ray adsorption (SEXAFS, NEXAFS) measurements on Cu(100) [7] and Cu(111) [6] yield a highly distorted adsorbate geometry. The C_2H_2 molecule, which is linear in gas phase, stabilizes on Cu(111) over a bridge site with the C–C axis almost parallel to the surface [3]. Two carbon centers are located near two adjacent threefold fcc and hcp hollow sites. This results in a C–C distance of the adsorbate, $d_{C-C}=1.48\pm0.10$ Å, which is greatly increased with respect to that of the free molecule, $d_{C-C}=1.20$ Å. A similar increase in d_{C-C} is concluded from C_2H_2 adsorption experiments on Cu(100) [7], Ni(110) [8] and Ni(111) [9,10]. More detailed information on the C_2H_2 adsorbate

distortion, including intramolecular d_{C-H} distances and C–C–H bending angles, requires measurements of the hydrogen positions at the surface which are very difficult in conventional diffraction experiments due to small cross sections. Therefore, no direct experimental data of hydrogen positions in adsorbed C_2H_2 seem to be available at present. Indirect evidence for bent C–H ends in adsorbed C_2H_2 may be obtained from infrared [11] as well as from X-ray [6] absorption experiments, but quantitative geometric results are still missing.

Ethylene (C_2H_4) adsorption on metal surfaces is also characterized by small adsorption energies and low temperatures required to stabilize adsorbate [4–7,12–16]. This molecule seems to bind differently depending on the substrate surface. On Ni(111) PED [4,5] as well as SEXAFS [7], experiments have identified major structural changes in C_2H_4 upon adsorption. The planar gas phase molecule stabilizes with its C–C axis parallel to the surface and its C centers bridging nearest-neighbor atom pairs (di-σ orientation, perpendicular to that found for C_2H_2 on Cu(111), Ni(111), see above). The C–C distance is increased by adsorption yielding d_{C-C}= 1.60±0.18 Å, compared to 1.34 Å for the free molecule. A similarly stretched C–C distance for adsorbed C_2H_4 was found in experiments on Cu(100) [7,13,14], Ag(100) [13,14], and Cu(110) [12]. In contrast, recent He atom scattering (HAS) and X-ray absorption (NEXAFS) experiments on Cu(111)–C_2H_4 [6] strongly suggest that the ethylene adsorbate is only weakly physisorbed without noticeable structural changes. This is also concluded from infrared absorption experiments on Cu(100)–C_2H_4 [11] and Cu(110)–C_2H_4 [16]. Further, hydrocarbon physisorption without restructuring was observed for Cu(111)–C_2H_6 [6].

Major molecular restructuring as a consequence of adsorbate–substrate binding has also been observed in other hydrocarbon/metal adsorbate systems. As an example we mention benzene adsorption. Here, diffuse low-energy electron-diffraction (DLEED) experiments on Pt(111)–C_6H_6 [17] have identified a Kekule distorted C_6H_6 adsorbate with alternating C–C distances varying between 1.49 and 1.64 Å. Further, recent X-ray absorption experiments on Pt(111)–C_6H_6 [18] suggest, for the adsorbate, an out-of-plane bending of the C–H bonds by ca. 30°.

2.2. Theoretical findings

The adsorption of C_2H_2 and C_2H_4 on transition metal surfaces has been discussed in various theoretical studies where both, electronic and geometric properties have been considered. These studies are based exclusively on the surface cluster approach where both semi-empirical [19] and ab-initio [20–27] techniques are used to determine the local electronic structure in the adsorbate system. In early ab-initio calculations [21,22], rather small $Me_nC_2H_2$, Me=Fe, Ni, Cu, n=1–3, clusters have been considered and the adsorbate geometry was varied within a very limited range. The authors assume a distorted C_2H_2 species in the clusters with the C–C distance being enlarged with respect to the free molecule value and the C–H ends bent away from the metal cluster (∠(C–C–H)=150°). For this geometry, the calculations yield a local adsorbate–substrate bond which can be characterized by a Dewar–Chatt–Duncanson donation mechanism [28–30]. The donation mechanism is well known from organometallic chemistry [30] and it its found to weaken the C–C bond of the adsorbate. Very similar conclusions concerning the distortion of the adsorbed molecule and adsorbate binding have been obtained in geometry optimizations of free $Cu_nC_2H_2$, n=1–4, compounds [23] as well for $Cu_nC_2H_2$, n=4, 7, 22 and for $Pd_nC_2H_2$, n=4, 7 surface clusters [24] simulating acetylene–metal adsorption. These studies are based on ab-initio Hartree–Fock wave functions with Møller–Plesset (MP2) type perturbative correlation corrections.

In recent ab-inito studies on a $Cu_7(4,3)C_2H_2$ surface cluster, simulating the Cu(111)–C_2H_2 adsorbate system, the adsorbate–substrate binding has been analyzed in some detail based on Hartree–Fock and configuration interaction (CI) [20] as well as density functional theory (DFT) [25] calculations. The calculations yield an optimized adsorbate geometry, where the C_2H_2 molecule is distorted increasing its C–C distance and bending the two CH ends away from the substrate. The binding analysis reveals a competitive scheme, where energy is required to distort the C_2H_2 molecule in the presence of the surface. The distortion energy is overcompensated by the energy gain due to local bond formation between the distorted adsorbate molecule and the substrate surface characterized by Dewar–Chatt–Duncanson donation [28,29]. The adsorbate distortion is connected with rehybridization and leads

to C–C bond weakening and to an increased intramolecular C–C distance. On the other hand, distortion leads to C_2H_2 adsorbate orbitals of lower symmetry which can couple more effectively with the substrate than those of the free linear molecule. This yields stronger binding between distorted C_2H_2 and the Cu substrate as compared to that of free C_2H_2. Thus, the competitive binding scheme and its geometric consequences are consistent with the experimental results for the Cu(111)–C_2H_2 adsorbate system [3–6].

Recently, the adsorption of ethylene at Cu(111) has been studied theoretically by a $Cu_7(4,3)C_2H_4$ cluster model including respective geometry optimization, where the electronic structure was determined within ab-initio Hartree–Fock and DFT approaches [25,26]. The results for the cluster geometry of lowest energy are completely analogous to those of the $Cu_7(4,3)C_2H_2$ cluster study [20,25]. The C_2H_4 adsorbate is found to stabilize over a Cu(111) bridge site with the C–C axis almost parallel to the surface and its C centers located near two adjacent threefold fcc and hcp hollow sites. In this lateral geometry, the C–C distance of the adsorbate is greatly increased with respect to that of the free molecule and CH_2 ends are bent away from the substrate by 50°. The binding analysis suggests a competitive scheme as for Cu(111)–C_2H_2 involving adsorbate distortion connected with rehybridization and C–C bond weakening and local adsorbate–substrate bond formation characterized by Dewar–Chatt–Duncanson donation. The concept of a dative adsorbate–substrate binding connected with C–C bond weakening for adsorbed C_2H_4 was also supported by DFT cluster studies on $Ni_{14}(C_2H_4)_2$ simulating the Ni(110)–C_2H_4 adsorbate system [8,27]. However, the results for the $Cu_7(4,3)C_2H_4$ cluster do not seem to be in agreement with experimental evidence for ethylene adsorption on transition metal surfaces described above. While there is no qualitative experimental information on the Cu(111)–C_2H_4 adsorption geometry, recent experiment [6] suggest ethylene physisorption without noticeable adsorbate restructuring. Further, for Ni(111)–C_2H_4 where experiments confirm a distorted C_2H_4 adsorbate [4,5] consistent with competitive binding, the adsorbate orientation (di-σ) differs from that obtained for the $Cu_7(4,3)C_2H_4$ cluster (cross-bridge orientation, the di-σ orientation does not yield a stable adsorbate in the cluster).

In view of the discrepancy between existing theoretical and experimental results for the Cu(111)–C_2H_4 adsorbate system, we re-examine in the present study the interaction of C_2H_2 and C_2H_4 with Cu(111) by cluster models where we consider a wider range of the adsorbate–substrate interaction.

3. Theoretical details

In the present work, the Cu(111) surface is simulated by a $Cu_7(4,3)$ substrate cluster of C_S symmetry. This cluster forms a compact section of the ideal Cu(111) surface with four atoms of the first and three atoms of the second surface layer and has proven to yield rather reliable electronic substrate properties for different adsorbates at the Cu(111) surface [31,32]. Further, separate calculations for acetylene adsorption on larger substrate clusters, up to $Cu_{22}(12,7,3)$ [20] and $Cu_{30}(14,8,8)$ [24], have shown that adsorbate geometries and bindings are only slightly affected if substrate clusters larger than $Cu_7(4,3)$ are considered. The Cu–Cu nearest-neighbor distance in $Cu_7(4,3)$ is set at the ideal bulk value, d_{Cu-Cu}=4.824 bohr, and is kept fixed in the calculations. The fixed geometry is justified since the cluster is expected to simulate a local environment at the Cu(111) surface rather than a finite (flexible) Cu_7 cluster. Acetylene adsorption is modeled by the C_2H_2 species placed on the C_S mirror plane perpendicular to the substrate surface (see Fig. 1). This cross-bridge orientation is suggested by the PED experiments on Cu(111)–C_2H_2 [3].

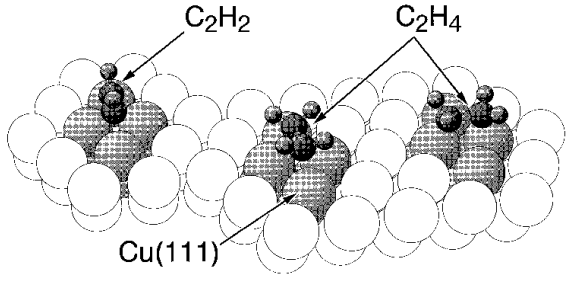

Fig. 1. Geometric structure of the $Cu_7(4,3)C_2H_2$ and $Cu_7(4,3)C_2H_4$ clusters used in the present study. The left part of the figure shows the cross-bridge orientation of the C_2H_2 adsorbate. For adsorbing C_2H_4, two surface orientations are considered: (middle) cross-bridge, and (right) di-σ. The light balls in the figure represent Cu substrate atoms (not included in the clusters) which are meant to illustrate the Cu(111) surface geometry.

Further, previous cluster studies on $Cu_7(4,3)C_2H_2$ [20,25] have shown that a full geometry optimization of the adsorbate yields the lowest cluster energy with the C_2H_2 on the C_S mirror plane. In the model calculations on ethylene adsorption two adsorbate orientations are considered (see Fig. 1). First, the C_2H_4 species is placed with its C–C axis on the C_S mirror plane of the substrate cluster, analogous to the cross-bridge geometry for $Cu(111)$–C_2H_2 described before. Second, the C_2H_4 species is placed with its C–C axis on a plane which points perpendicular to the substrate and includes a Cu–Cu nearest-neighbor pair. This orientation (di-σ) is found, in PED experiments, for the $Ni(111)$–C_2H_4 adsorbate system [4,5].

The electronic structure and derived properties of the clusters are obtained with ab-initio density-functional theory (DFT) method [33,34] using the local spin density approximation (LSDA) for exchange and correlation, based on the Vosko–Wilk–Nusair functional [35]. Gradient corrected (GGA) exchange-correlation functionals beyond LSDA can improve the cluster binding-energy results. Therefore, total energies for characteristic cluster geometries are also evaluated using the GGA-I functional [36]. The basis sets of contracted Gaussian orbitals (CGTO's) are all-electron type and are taken from free atom DFT optimizations [37]. Full geometry optimizations of the adsorbates in the $Cu_7(4,3)C_2H_2$ and $Cu_7(4,3)C_2H_4$ clusters based on total energy minimizations have been reported previously [20,25,26]. In the present study, we perform additional restricted optimizations. Here, the adsorbates are fixed with their C–C axes parallel to the surface at different positions z above the substrate (z denoting the perpendicular distance between the first substrate layer and the C–C axis) and their adsorbate geometry is optimized locally. This yields total energy curves $E(z)$ of the clusters characterizing the adsorbate–substrate interaction along an adiabatic model reaction path which can give information about different adsorbate states in the system, as will be discussed below.

4. Results and discussion

4.1. Acetylene adsorption

Fig. 2 shows a total energy curve $E(z)$ for the $Cu_7(4,3)C_2H_2$ cluster along the adiabatic adsorption path obtained from the restricted optimization described in Section 3. Here $E(z)$ has been shifted such that the energy zero coincides with the total energy at infinite adsorbate–substrate separation, i.e. $E(z\rightarrow\infty)=0$ characterizing the free, linear molecule state (A). Obviously, there is an attractive interaction between the C_2H_2 adsorbate and the $Cu_7(4,3)$ substrate already for large distances z along the adsorption path with an outer energy minimum (B) at z=5 bohr. In this minimum (B), the adsorbate is weakly bound to the substrate and its geometry is almost identical to that of the free C_2H_2 molecule, as can be seen from the inset of Fig. 2 and from the quantitative results listed in Table 1. The molecule increases its C–C and C–H bond distances by only 0.01 and 0.02 bohr, respectively, and its CH ends are bent away from the linear geometry by 1°. Further, orbital analyses together with Mulliken populations listed in Table 2(a) yield only minor charge rearrangements in the adsorbate which accumulates an overall small positive charge (+0.22 au). This indicates that the weak adsorbate–substrate interaction at the outer energy minimum (B) has almost no effect on the electronic structure of the adsorbate and must, therefore, be attributed to a weak polarization interaction.

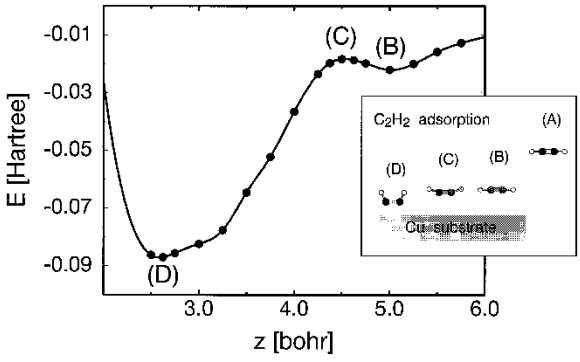

Fig. 2. Total energy curve $E(z)$ for the $Cu_7(4,3)C_2H_2$ cluster along an adiabatic adsorption path obtained from a restricted optimization (see text). The inset visualizes the geometry of the adsorbate at four selected points of the path: (A) free C_2H_2 molecule, (B) outer minimum, (C) barrier, and (D) inner minimum.

For distances z below the value of the outer energy minimum (B) the C_2H_2 adsorbate starts to distort the total energy curve $E(z)$ slightly. Thus, the gain in total energy due to weak polarization attraction (dominating at large adsorbate–substrate distances) is overcompensated by the energy required to distort the

Table 1
Geometry of the $Cu_7(4,3)C_2H_2$ cluster for selected points along the adiabatic adsorption path described in the text. Here, z_{C-Cu} denotes the perpendicular distance between the first substrate layer and the C–C axis of C_2H_2 while d_{C-C}, d_{C-H}, and ϑ(CCH) refer to intramolecular distances and angles in the adsorbate. All distances are given in bohrs and angles in degrees

	z_{C-Cu}	d_{C-C}	d_{C-H}	ϑ(CCH)
(A) Free molecule	—	2.30	2.05	180.0
(B) Outer minimum	5.00	2.31	2.07	179.1
(C) Barrier	4.50	2.35	2.08	161.0
(D) Inner minimum	2.65	2.65	2.10	116.0
Full optimization	2.63/2.77	2.65	2.10	116.3/119.8
Experiment [3]	2.61/2.72±0.06	2.80±0.19	—	—

Table 2
Mulliken populations q of all adsorbate centers and total adsorbate charges Q in the model clusters (a) $Cu_7(4,3)C_2H_2$ and (b) $Cu_7(4,3)C_2H_4$ for selected points along the adiabatic adsorption path. For a definition of points (A)–(D) see text and Table 1

(a) *$Cu_7(4,3)C_2H_2$*

	q(C1)	q(C2)	q(H1)	q(H2)	$Q(C_2H_2)$
(A) Free molecule	6.27	6.27	0.73	0.73	+0.00
(B) Outer minimum	6.23	6.16	0.71	0.68	+0.22
(C) Barrier	6.25	6.18	0.71	0.68	+0.18
(D) Inner minimum	6.37	6.37	0.73	0.73	−0.20

(b) *$Cu_7(4,3)C_2H_4$*

	q(C1)	q(C2)	q(H1/H2)	q(H3/H4)	$Q(C_2H_4)$
(A) Free molecule	6.46	6.46	0.77	0.77	+0.00
(B) Outer minimum	6.45	6.47	0.72	0.70	+0.24
(C) Barrier	6.51	6.55	0.68	0.66	+0.25
(D) Inner minimum	6.78	6.80	0.65	0.64	−0.16

adsorbate. This process continues until a distance z=4.50 bohr, where $E(z)$ reaches a local maximum (C). At this maximum, which defines a transition state and lies 0.10 eV above the outer energy minimum (B), the intramolecular distances d_{C-C} and d_{C-H} differ from those of minimum (B) by only 0.04 and 0.01 eV. However, the CH ends are bent by 19° from the linear geometry (ϑ(CCH)=161.0°, see Table 1). For distances z smaller than that of the barrier (C), the total energy curve $E(z)$ decreases dramatically until it reaches a local minimum (inner minimum (D) at z=2.65 bohr and 1.77 eV below the outer minimum (B)) beyond which $E(z)$ rises steeply. The energy decrease between (C) and (D) is combined with major restructuring of the adsorbate. At the inner minimum (D), the C–C distance adsorbate is increased by 0.35 bohr, the C–H distance by 0.05 bohr, and the CH ends are bent by 64° with respect to the free molecule geometry (see Table 1). Further, the adsorbate assumes a small negative charge (−0.20 au., see Table 2(a)). Obviously, the changed molecular geometry allows for strong adsorbate–substrate binding which can overcome the energy required to distort the C_2H_2 molecule.

In order to study the effect of exchange correlation functionals beyond LSDA, the $Cu_7(4,3)C_2H_2$ cluster energy is re-evaluated for all characteristic geometries, (A) to (D), at the adiabatic adsorption path, where the gradient corrected GGA-I functional [36] is applied. Table 3(a) lists adsorbate binding energies E_b, computed from respective total energy differences, for geometries (B) to (D), where E_b is determined using both the LSDA and the GGA-I functional. Table 3(a) also contains values for the barrier height, Δ_{BC}, between the outer minimum (B) and barrier (C), computed with both approximations. As expected, the GGA-I based binding energy values are, for all geometries well above those of the LSDA treatment which

Table 3
Adsorbate binding energies E_b of the clusters (a) $Cu_7(4,3)C_2H_2$ and (b) $Cu_7(4,3)C_2H_4$ for selected points along the adiabatic adsorption path. For a definition of points (B)–(D), see text and Tables 1 and 2. The quantity Δ_{BC} gives the barrier height between points (B) and (C). Results based on both the local spin density (LSDA) and the generalized gradient approximation (GGA-I) are listed. All energies are given in eV

(a) *$Cu_7(4,3)C_2H_2$*	E_b (B)	E_b (C)	E_b (D)	Δ_{BC}
LSDA	−0.60	−0.50	−2.37	0.10
GGA-I	−0.17	−0.01	−1.02	0.16
(b) *$Cu_7(4,3)C_2H_4$*				
SDA	−0.78	−0.43	−0.78	0.35
GGA-I	−0.23	+0.36	+0.34	0.59

brings the theoretical results, closer to experiment. Further, the GGA-I based barrier height Δ_{BC} is larger than the LSDA result. However, the GGA-I treatment does not alter the qualitative features of the adiabatic adsorption path discussed above where LSDA results are used.

The binding in free linear C_2H_2 is described by a C–C triple bond and C–H bonds derived from *sp* hybridization at the carbon centers. The distortion of the molecule by bending its CH ends (to yield the adsorbate shape) results in a bond situation which is typical for sp^2 hybridization and may be visualized as creating an incomplete C_2H_4 molecule with one hydrogen missing on each side. Thus, the molecule distortion leads to an effective transition from a C≡C triple to weaker double bond and from *sp* to sp^2 hybridization near the adsorbate C centers. The sp^2 hybrid orbitals are not fully saturated, making the C centers reactive and available for binding with the metal surface. Thus, the binding situation of the inner minimum (D) is characterized by competing effects where energy is needed to distort the adsorbate and gained by an increased binding between the distorted adsorbate and the substrate. This competitive binding scheme has been discussed previously [20,25] in great details, based on orbital and population analyses. The analysis has shown that the Dewar–Chatt–Duncanson type dative binding is stronger for the distorted than for the linear C_2H_2 adsorbate and that *sp* to sp^2 rehybridization at the carbon centers of the distorted adsorbate can explain the increased C–C binding distance.

Table 1 also contains results from a full geometry optimization of the adsorbate in the $Cu_7(4,3)C_2H_2$ cluster of C_S symmetry [25]. Here, the adsorbate stabilizes in a geometry very close to that of the inner minimum (D) of the restricted optimization. The intramolecular distances, $d_{C–C}$ and $d_{C–H}$, are almost identical for the two optimizations while the full geometry optimization yields slightly different adsorbate–substrate distances for the two C centers of C_2H_2 combined with different CH bending angles. Calculations yield $z_{Cl–Cu}$=2.63 bohr for Cl near the fcc hollow and $z_{C2–Cu}$=2.77 bohr for C2 near the hcp hollow site on Cu(111) with bending angles ϑ(C2C1H)=116.3° and ϑ(C1C2H)=119.8°. This corresponds to a distorted C_2H_2 adsorbate with its C–C axis inclined at 3° with respect to the substrate surface. The nonequivalence of the two adsorbate C centers is explained by the substrate environment differing somewhat near adjacent fcc and hcp hollow sites at the substrate surface. However, the comparison shows altogether, that the present restricted optimizations are also able to account for the fully optimized adsorbate geometry of the $Cu_7(4,3)C_2H_2$ cluster.

In addition to theoretical results, Table 1 includes experimental PED data for the adsorbate geometry of the Cu(111)–C_2H_2 system [3]. These results are in very good agreement with the theoretical cluster results from the full optimization and from that of the inner minimum (D). The calculations reflect the experimentally verified adsorbate orientation at the Cu(111) surface and reproduce the C–C distance of the adsorbate as well as the C–Cu distances of the two nonequivalent adsorbate C centers rather well. Unfortunately, calculated C–H distance values and CCH bending in the C_2H_2 adsorbate, which are important ingredients to substantiate the theoretical bond formation scheme, cannot be compared with experiment since hydrogen positions have not been evaluated by PED [3]. However, the experimental results together with the present theoretical cluster data suggest strongly that C_2H_2 adsorption on Cu(111) can be described by a competitive binding scheme reflecting the inner minimum (D) of the calculations. In contrast, the outer minimum (B), describing physisorption, has not been observed so far by experiment. Very recent theoretical cluster studies on hydrocarbon adsorption at Cu surfaces [38] confirm the present findings and, in addition, show that the two adsorption states discussed

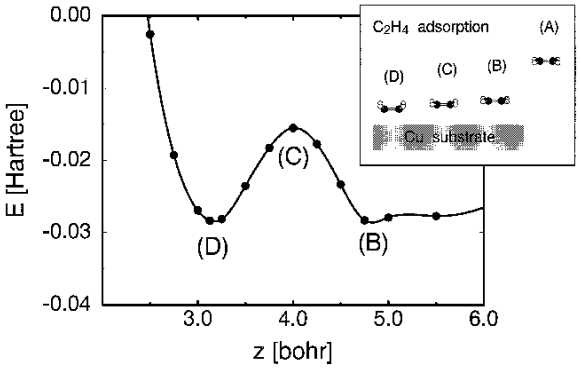

Fig. 3. Total energy curve $E(z)$ for the $Cu_7(4,3)C_2H_4$ cluster along an adiabatic adsorption path obtained from a restricted optimization with the C_2H_4 in cross-bridge orientation (see text). The inset visualizes the geometry of the adsorbate at four selected points of the path: (A) free C_2H_4 molecule, (B) outer minimum, (C) barrier, and (D) inner minimum.

in the present study can be interpreted in terms of differently prepared bond states where excited states of the adsorbate are involved.

4.2. Ethylene adsorption

Restricted optimizations for the $Cu_7(4,3)C_2H_4$ cluster are performed for two orientations of the C_2H_4 adsorbate at the surface, di-σ (bridging a Cu–Cu nearest-neighbor pair at Cu(111)) and cross-bridge (analogous to that of $Cu_7(4,3)C_2H_2$), see Fig. 1. The calculations for the di-σ orientation yield a repulsive total energy curve $E(z)$ with no binding minimum [26]. Thus, di-σ oriented ethylene does not stabilize on the $Cu_7(4,3)$ cluster which could suggest that the di-σ oriented C_2H_4 adsorbate may not be observed on the Cu(111) surface. In contrast, the $E(z)$ results for C_2H_4 approaching the $Cu_7(4,3)$ substrate in a cross-bridge orientation are qualitatively very similar to those of the $Cu_7(4,3)C_2H_2$ cluster discussed above. This becomes obvious from Fig. 3 which shows the total energy curve $E(z)$ obtained for $Cu_7(4,3)C_2H_4$ for the cross-bridge oriented adsorbate. As before, $E(z)$ has been shifted such that $E(z\rightarrow\infty)=0$, where $z\rightarrow\infty$ characterizes the free planar molecule state (A). Note that preliminary results from restricted optimizations on $Cu_7(4,3)C_2H_4$ have been communicated before (cf. $E(z)$ curve in Fig. 3 of Ref. [26]). However, the physical implications of $E(z)$ have not been pointed out in detail previously [26].

Fig. 3 shows an attractive interaction between C_2H_4 and the $Cu_7(4,3)$ substrate for large distances z along the adsorption path with an outer energy minimum (B) at z=4.81 bohr. Note that the weak polarization interaction between C_2H_4 and $Cu_7(4,3)$ seems to be effective at larger distances compared to those of the interaction between C_2H_2 and $Cu_7(4,3)$. The origin of this behavior is not obvious and may be partly due to different polarizabilities of the two adsorbates. However, while this point needs to be studied in greater detail, it does not influence the present conclusions. At minimum (B), the adsorbate geometry is very close to that of the free C_2H_4 molecule as can be seen from the inset of Fig. 3 and from the quantitative results listed in Table 4. The molecule increases its C–C bond distance by only 0.04 bohr and the HCH angles are almost unaffected (ϑ(CCH)=120.1°) while the CH_2 ends of C_2H_4 are bent away from the planar

Table 4
Geometry of the $Cu_7(4,3)C_2H_4$ cluster for selected points along the adiabatic adsorption path described in the text. Here, z_{C-Cu} denotes the perpendicular distance between the first substrate layer and the C–C axis of C_2H_4 while d_{C-C}, d_{C-H}, ϑ(HCH), and $\vartheta(CCH_2)$ refer to intramolecular distances and angles in the adsorbate. All distances are given in bohrs and angles in degrees. Note that the experimental data refer to the Ni(111)–C_2H_4 system [4,5]

	z_{C-Cu}	d_{C-C}	d_{C-H}	ϑ(HCH)	$\vartheta(CCH_2)$
(A) Free molecule	—	2.52	2.08	120.0	180.0
(B) Outer minimum	4.81	2.56	2.08	120.1	172.1
(C) Barrier	4.00	2.61	2.08	120.1	161.3
(D) Inner minimum	3.12	2.88	2.09	113.6	133.4
Full optimization	3.13/3.13	2.88	2.09	114.0	132.8/133.9
Experiment [4,5]	(3.59±0.04)	(3.02±0.34)	—	—	—

geometry by 7.8°. The latter is quantified by $\vartheta(CCH_2)$, describing the angle between the C–C axis and each of the CH_2 planes of the adsorbate. Orbital analyses together with Mulliken populations listed in Table 2(b) yield only small charge rearrangements in the C_2H_4 adsorbate which becomes positively charged by +0.24 au. This indicates, analogous to the acetylene adsorbate, a weak adsorbate–substrate interaction at the outer energy minimum (B) which hardly affects the electronic structure of the adsorbate and must be due to a weak polarization coupling rather than chemical-bond formation.

For distances z, smaller than the value of the outer energy minimum (B), the C_2H_4 adsorbate starts to distort which is combined with increasing $E(z)$ values. This means that, in analogy to the C_2H_2 adsorbate result, the total energy gain due to weak polarization attraction at large adsorbate–substrate distances is balanced by the energy required to distort the adsorbate with the latter becoming more important at smaller distances. The total energy continues to increase until a distance z=4.00 bohr, where $E(z)$ reaches a local maximum (C). This maximum defines a transition state where the intra adsorbate distance $d_{C–C}$ is slightly increased (by 0.04 bohr relative to geometry (B)) while the $d_{C–H}$ distance and the HCH angles remain unchanged. In contrast, the CH_2 ends of C_2H_4 are bent away from the planar geometry by a sizeable amount of 18.7° ($\vartheta(CCH_2)$=161.3°, see Table 4). The barrier height for C_2H_4 defined by the difference in total energy between the physisorption minimum (B) and the barrier top (C) yields 0.35 eV which is more than three times as large as the corresponding value for the C_2H_2 adsorbate (0.10 eV). Obviously, the distortion energy connected with the movement from (B) to (C) is much larger for C_2H_4 than for the C_2H_2 adsorbate. As a result, the adsorbing ethylene molecule requires more energy to overcome barrier (C) compared to adsorbing acetylene which may make the barrier crossing less likely for C_2H_4.

For distances z below that of barrier (C), the total energy curve $E(z)$ for $Cu_7(4,3)C_2H_4$ decreases and reaches a local minimum, inner minimum (D), at z=3.12 bohr. The $E(z)$ value at this minimum lies only 0.02 eV below that of the outer minimum (B). The energy decrease between (C) and (D) is, as for acetylene adsorption, accompanied by major restructuring of the C_2H_4 adsorbate. At the inner minimum (D), the C–C distance of the adsorbate is increased by 0.36 bohr, the C–H distances by 0.01 bohr, and the CH_2 ends are bent 47° with respect to the free molecule geometry while the HCH angles are decreased by only 6°, see Table 4. In addition, the adsorbate becomes negatively charged (−0.16 au., see Table 2(b)). This strongly changed adsorbate geometry of C_2H_4 at the inner minimum (D) suggests an adsorbate–substrate binding scheme which is qualitatively identical to that of C_2H_2.

The influence caused by exchange correlation functionals beyond LSDA is examined analogous to the acetylene adsorbate system by computing $Cu_7(4,3)C_2H_4$ cluster total energies for all characteristic geometries (A) to (D) at the adiabatic adsorption path using the gradient corrected GGA-I functional [36]. Table 3(b) lists adsorbate binding energies E_b, computed from respective total energy differences, for geometries (B) to (D), where E_b is determined using both, LSDA and the GGA-I functional. Note that the definition of E_b yields negative values if the adsorbate binds to the substrate while positive values point at metastability, or instability, with respect to the separated adsorbate limit (A). Table 3(b) includes also values for the barrier height, Δ_{BC}, between the outer minimum (B) and the barrier (C). As for $Cu_7(4,3)C_2H_2$, the GGA-I based binding energy values are, for all geometries, above those of the LSDA treatment. In addition, the inner minimum (D) describes a metastable state with an energy only slightly below that of barrier (C). Further, the GGA-I based barrier height Δ_{BC} is increased over the LSDA result. This may make the inner minimum (D) difficult to reach in the experiment. Altogether, the GGA-I treatment suggests a double minimum binding curve as found in the LSDA results where, however, the relative energy position of the two minima differs for the two approximations.

The binding in free planar C_2H_4 is described by a C=C double bond and C–H bonds derived from sp^2 hybridization at the carbon centers. The distortion of the C_2H_4 molecule, by bending its CH_2 ends (to yield the adsorbate geometry), results in a bond formation which is typical for sp^3 hybridization and may be visualized as creating an incomplete C_2H_6 molecule with one hydrogen missing on each side. Thus, the molecule distortion leads to an effective transition from a C=C double to a weaker single bond and from

sp^2 to sp^3 hybridization near the adsorbate C centers. The sp^3 hybrid orbitals are not fully saturated making the C centers reactive and available for binding with the metal surface. Altogether, adsorbate binding at the inner minimum (D) is characterized by competing effects where energy is required to distort the adsorbate and is gained by an increased Dewar–Chatt–Duncanson type dative binding between the distorted adsorbate and the substrate. In addition, orbital and population analyses for $Cu_7(4,3)C_2H_4$ show [25,26] that sp^2 to sp^3 rehybridization at the carbon centers of the distorted adsorbate can explain the increased C–C binding distance at the inner minimum (D). The results from a full geometry optimization of the C_2H_4 adsorbate in $Cu_7(4,3)C_2H_4$ [25] assuming C_S symmetry and cross-bridge orientation are included in Table 4. They show that the adsorbate stabilizes in a geometry very close to that of the inner minimum (D) of the restricted optimization which was concluded also from the calculations on acetylene adsorption. Thus, the present restricted optimizations are able to account also for the fully optimized adsorbate geometry of the $Cu_7(4,3)C_2H_4$ cluster.

So far, the present theoretical geometry data for ethylene adsorption cannot be compared quantitatively with experimental values since explicit geometry parameters have not been measured for the Cu(111)–C_2H_4 system. Experimental PED data for the adsorbate geometry of the Ni(111)–C_2H_4 system [4,5], which are included in Table 4, confirm the increased C–C distance of the C_2H_4 adsorbate obtained in the cluster calculations for the inner minimum (D). However, the Ni(111)–C_2H_4 measurements find the adsorbate in a di-σ orientation which is excluded in the present model calculations for Cu(111). This discrepancy is most likely due to different *d* electron participation in the surface binding as a result of the open shell $3d^9$ structure of Ni compared to a closed shell $3d^{10}$ for Cu. Recent He atom scattering (HAS) and X-ray absorption (NEXAFS) experiments on Cu(111)–C_2H_4 [6] give strong indications that the ethylene adsorbate is only weakly physisorbed without noticeable structural changes. This is consistent with the present theoretical cluster results for the outer minimum (B), whereas C_2H_4 adsorption on Cu(111) described by competitive binding at the inner minimum (D) has not been confirmed so far by experiment.

5. Conclusions

The nature of hydrocarbon binding and reactions on metal surfaces is very complex and involves, in general, different kinds of molecularly and dissociatively adsorbed species. Here, the adsorbate molecules may be physisorbed (without significant changes in their electronic structure), molecularly chemisorbed (connected with chemical surface binding), or may transform to chemisorbed/physisorbed products where energetic barriers separate the different sorption states. The heights of the barriers, together with relative bond strength of the different sorption states, will determine respective reaction paths and final products.

The present DFT cluster model studies reveal interesting details of the binding of acetylene and ethylene at the Cu(111) surface which can be relevant also for other metal–hydrocarbon adsorbate systems. The calculations indicate, for both Cu(111)–C_2H_2 and Cu(111)–C_2H_4, two local potential minima, denoted by (B) and (D), which refer to adsorbate states of a different character and are separated by a barrier. The potential minimum belonging to the smaller adsorbate–substrate distance (‘inner minimum’ (D)) is described, in both systems, by competitive binding and a strongly distorted adsorbate. In addition, the present calculations yield, for both systems, a potential minimum at larger adsorbate–substrate distance (‘outer minimum’ (B)) which represents a weakly physisorbed state, where the hydrocarbon molecule is not affected in its geometry. There are three main differences in the theoretical interaction potentials which distinguish between the Cu(111)–C_2H_2 and Cu(111)–C_2H_4 systems and shed some light on the different adsorption behavior of the two adsorbates. First, the outer physisorption minimum (B) for ethylene is located closer to the surface and lies energetically somewhat lower than that of acetylene which can be explained by different polarizabilities of the two adsorbates. Second, the inner potential minimum (D) is substantially lower than that of the outer minimum (B) for acetylene (cf. Fig. 2). This contrasts with ethylene, where the total energies of the inner and outer minima assume almost the same value in the LSDA treatment, see Fig. 3, while the GGA-I calculations place the inner minimum well above the outer. The adsorbate–substrate interaction near the minimum (D) is described for both the systems by a

competitive scheme, where energy is required to distort the adsorbate molecule but is gained by increased Dewar–Chatt–Duncanson type dative binding. Previous calculations [25] have shown that the distortion energy is larger for C_2H_2 than for C_2H_4 which, together with the present results, suggests that the increased dative binding of distorted ethylene is less effective than that of acetylene. Third, the calculated energy barrier, separating the inner from the outer minimum, is three times smaller for adsorbing acetylene than for ethylene. As a consequence, acetylene approaching the Cu(111) surface may stabilize in the outer physisorption minimum (B) only shortly thereafter it moves closer to the inner chemisorption minimum (D) overcoming the relatively small energy barrier and gaining substantial binding energy. In contrast, ethylene approaches the Cu(111) surface and stabilizes in the outer physisorption minimum (B) from where a transition to the inner minimum (D) is much more difficult due to the higher energy barrier and results in only little binding energy gain (LSDA results) or may even require energy (GGA-I results). These results are consistent with the experimental findings of competitive binding for Cu(111)–C_2H_2 [3], while for Cu(111)–C_2H_4, so far physisorption [6] is observed. However, the present theoretical results suggest that both adsorbate states exist in the real systems and may be observed by appropriate sample preparation.

Acknowledgements

Stimulating discussions with Profs. A.M. Bradshaw, C. Wöll, and L.G.M. Pettersson are gratefully acknowledged.

References

[1] K. Hermann, K. Freihube, T. Greber, A. Böttcher, R. Grobecker, D. Fick, G. Ertl, Surf. Sci. 313 (1994) L806.
[2] T. Greber, K. Freihube, R. Grobecker, A. Böttcher, K. Hermann, G. Ertl, Phys. Rev. B50 (1994) 8755.
[3] S. Bao, K.-M. Schindler, P. Hofmann, V. Fritzsche, A.M. Bradshaw, D.P. Woodruff, Surf. Sci. 291 (1993) 295.
[4] S. Bao, P. Hofmann, K.M. Schindler, V. Fritzsche, A.M. Bradshaw, D.P. Woodruff, M.C. Asensio, J. Phys.: Condens. Matter 6 (1994) L93.
[5] S. Bao, P. Hofmann, K.M. Schindler, V. Fritzsche, A.M. Bradshaw, D.P. Woodruff, C. Casado, M.C. Asensio, Surf. Sci. 323 (1995) 19.
[6] D. Fuhrmann, D. Wacker, K. Weiss, K. Hermann, M. Witko, C. Wöll, J. Chem. Phys., in press.
[7] D. Arvanitis, L. Wenzel, K. Baberschke, Phys. Rev. Lett. 59 (1987) 2435.
[8] M. Weinelt, W. Huber, P. Zebisch, H.-P. Steinrück, P. Ulbricht, U. Birkenheuer, J.C. Boettger, N. Rösch, J. Chem. Phys. 102 (1995) 9709.
[9] L. Hammer, T. Hertlein, K. Müller, Surf. Sci. 178 (1986) 693.
[10] S. Lehwald, H. Ibach, Surf. Sci. 89 (1979) 425.
[11] N. Sheppard, Ann. Rev. Phys. Chem. 39 (1988) 589.
[12] O. Schaff, A.P.J. Stampfl, P. Hofmann, S. Bao, K.-M. Schindler, V. Fritsche, A.M. Bradshaw, Surf. Sci. 343 (1995) 201.
[13] H. Rabus, D. Arvanitis, M. Domke, K. Baberschke, J. Chem. Phys. 96 (1992) 1560.
[14] D. Arvanitis, H. Rabus, L. Wenzel, K. Baberschke, Z. Phys. D. (Atoms, Molecules and Clusters) 11 (1989) 219.
[15] R. Raval, Surf. Sci., 331–333 (1995) 1.
[16] E. Cooper, R. Raval, Surf. Sci., 331–333 (1995) 94.
[17] A. Wander, G. Held, R.Q. Hwang, G.S. Blackman, M.L. Xu, P. de Andres, M.A. Van Hove, G.A. Somorjai, Surf. Sci. 249 (1991) 21.
[18] C. Mainka, P.S. Bagus, A. Shertel, T. Strunskus, M. Grunze, C. Wöll, Surf. Sci. 341 (1995) L1055.
[19] A.B. Anderson, J. Am. Chem. Soc. 99 (1977) 696.
[20] K. Hermann, M. Witko, Surf. Sci. 337 (1995) 205.
[21] P. Geurts, A. van der Avoird, Surf. Sci. 102 (1981) 185.
[22] P. Geurts, A. van der Avoird, Surf. Sci. 103 (1981) 416.
[23] M. Böhme, T. Wagner, G. Frenking, J. Organomet. Chem. 520 (1996) 31.
[24] A. Clotet, G. Pacchioni, Surf. Sci. 346 (1996) 91.
[25] K. Hermann, M. Witko, A. Michalak, Z. Phys. Chem. 197 (1996) 219.
[26] A. Michalak, M. Witko, K. Hermann, J. Mol. Catal. 119 (1997) 213.
[27] M. Weinelt, W. Huber, P. Zebisch, H.-P. Steinrück, M. Pabst, N. Rösch, Surf. Sci. 271 (1992) 539.
[28] M.J.S. Dewar, Bull. Soc. Chim. France 18 (1951) C79.
[29] J. Chatt, L.A. Duncanson, J. Chem. Soc., (1953) 2939.
[30] M.R. Albert, J.T. Yates, The Surface Scientist's Guide to Organometallic Chemistry, ACS Publishing, Washington. 1987.
[31] K. Hermann, M. Witko, L.G.M. Pettersson, P. Siegbahn, J. Chem. Phys. 99 (1993) 610.
[32] M. Witko, K. Hermann, J. Chem. Phys. 101 (1994) 10173.
[33] J.K. Labanowski, J.W. Anzelm (Eds.), Density Functional Methods in Chemistry, Springer-Verlag, New York 1991.
[34] For the present calculations, the DeMon program system was used. DeMon was developed by A. St-Amant, D. Salahub (University of Montreal) and is available from these authors.
[35] S.H. Vosko, L. Wilk, M. Nusair, Can. J. Phys. 58 (1980) 1200.
[36] J.P. Perdew, Y. Wang, Phys. Rev. B46 (1992) 6671.
[37] N. Godbout, D.R. Salahub, J. Andzelm, E. Wimmer, Can. J. Phys. 70 (1992) 560.
[38] L. Triguero, L.G.M. Pettersson, B. Minaev, H. Ågren, J. Chem. Phys. 108 (1998) 1193.